Integrated miR-34a/SIRT1 Axis Links Inflammation, Oxidative Stress, and Endothelial Dysfunction to Cardiovascular Risk in Type 2 Diabetes

Fábio Morato de Oliveira *, Fermino Sanches Lizarte Neto, Eduardo Vignoto Fernandes, Mayara Bocchi, David Michel de Oliveira, Carla Silva Siqueira

Posted Date: 19 March 2026

doi: 10.20944/preprints202603.1509.v1

Keywords: microRNA; cardiovascular diseases; noncommunicable diseases; metabolic diseases

 doi:10.20944/preprints202603.1509.v1

Article

Integrated miR-34a/SIRT1 Axis Links Inflammation, Oxidative Stress, and Endothelial Dysfunction to Cardiovascular Risk in Type 2 Diabetes

Fábio Morato de Oliveira [1,*], Fermino Sanches Lizarte Neto [2], Eduardo Vignoto Fernandes [3], Mayara Bocchi [3], David Michel de Oliveira [3] and Carla Silva Siqueira [4]

[1] Laboratory of Human & Medical Genetics, Federal University of Jataí, Jataí-GO, Brazil
[2] Faculty of Medicine of Ribeirão Preto, University of São Paulo – USP, Ribeirão Preto, SP, Brazil
[3] Laboratory of Immunometabolism, Nutrition and Exercise (LABINE), Federal University of Jataí, Jataí-GO, Brazil
[4] Laboratory of Oral Pathology, Faculty of Odontology, Federal University of Uberlândia, Uberlândia – Minas Gerais, Brazil
* Correspondence: fabiomorato@ufj.edu.br

Abstract

Type 2 diabetes mellitus (T2DM) is a major driver of cardiovascular disease (CVD), yet current risk stratification tools fail to capture underlying molecular dysregulation. This study aimed to characterize an integrated molecular signature associated with cardiovascular risk in T2DM. A total of 128 individuals (96 T2DM and 32 controls) were evaluated. Circulating miR-34a expression was quantified by RT–qPCR, and protein biomarkers including SIRT1, inflammatory markers (IL-6, TNF-α, hs-CRP), oxidative stress markers (MDA, total antioxidant capacity), and endothelial dysfunction markers (VCAM-1, ICAM-1) were measured by ELISA. Cardiovascular risk was assessed using the Framingham Risk Score. miR-34a expression was significantly elevated in T2DM, particularly in individuals with high cardiovascular risk ($p < 0.001$). This was accompanied by reduced SIRT1 levels and a progressive increase in inflammatory, oxidative, and endothelial dysfunction markers. Integrated analysis revealed strong correlations between miR-34a upregulation, SIRT1 suppression, and systemic pathophysiological alterations. Multivariate regression identified miR-34a, SIRT1, IL-6, and MDA as independent predictors of high cardiovascular risk. A combined biomarker model demonstrated excellent discriminative performance (AUC = 0.92), outperforming individual markers. These findings support the existence of a coordinated miR-34a/SIRT1-driven molecular axis linking inflammation, oxidative stress, and endothelial dysfunction to cardiovascular risk in T2DM. This integrated biomarker approach may improve risk stratification and support precision cardiometabolic medicine.

Keywords: microRNA; cardiovascular diseases; noncommunicable diseases; metabolic diseases

1. Introduction

Cardiovascular disease represents the most common complication of diabetes in individuals diagnosed with type 2 diabetes mellitus (T2DM), being two to four times more likely to develop cardiovascular disease, compared to those without diabetes [1,2]. Even prediabetes is associated with an elevated risk of vascular complications [3,4]. Chronic hyperglycemia leads to the generation of advanced glycation end products and reactive oxygen species. These contribute to endothelial dysfunction and vascular inflammation, both hallmarks of atherosclerosis [5].

MicroRNA-34a (miR-34a) is a small, non-coding RNA molecule that plays a significant role in the regulation of gene expression [6]. In the context of diabetes mellitus, particularly T2DM, miR-34a has been implicated in various pathophysiological processes, including insulin resistance, β-cell

 doi:10.20944/preprints202603.1509.v1

dysfunction, and vascular complications [7]. Studies have demonstrated that miR-34a expression is upregulated in the pancreatic islets of diabetic mice. By downregulating *BCL-2*, miR-34a promotes β-cell apoptosis, leading to reduced insulin secretion. miR-34a also modulates insulin signaling by targeting components of the insulin receptor signaling pathway, such as IRS-1 (*Insulin Receptor Substrate 1*) [8,9]. Overexpression of miR-34a has been shown to impair insulin secretion and promote apoptosis in β-cells by targeting key regulatory proteins such as *BCL-2* and *SIRT1* [8–10]. This dysregulation contributes to the progressive decline in β-cell function observed in T2DM [7,8].

Vascular complications are a major concern in diabetes, leading to increased morbidity and mortality [11]. miR-34a has been identified as a contributor to endothelial dysfunction, a precursor to vascular complications [12]. In diabetic conditions, elevated levels of miR-34a suppress the expression of *SIRT1*, a protein that protects against endothelial dysfunction [10]. This suppression results in increased oxidative stress and inflammation within the vascular endothelium [10,11]. Given its involvement in key diabetic processes, miR-34a presents a potential therapeutic target[8,9]. Additionally, miR-34a inhibitors may protect β-cells from apoptosis, preserving insulin secretion and delaying the progression of in T2DM [7,8]. Targeting miR-34a offers a promising avenue for therapeutic intervention, aiming to mitigate the progression and complications associated with diabetes.

In the present study, we aimed to characterize the integrated molecular signature underlying cardiovascular risk in individuals with type 2 diabetes mellitus (T2DM). We investigated circulating miR-34a expression and its regulatory target SIRT1 in conjunction with inflammatory mediators (IL-6, TNF-α, hs-CRP), oxidative stress indicators (MDA, total antioxidant capacity), and endothelial dysfunction markers (VCAM-1, ICAM-1). We evaluated their interrelationships and their association with glycemic control and cardiovascular risk categories defined by the Framingham Risk Score. Therefore, we hypothesized that circulating *miR-34a* expression is associated with cardiovascular risk in individuals with T2DM and reflects underlying metabolic and inflammatory dysregulation. This study aimed to evaluate *miR-34a* expression and its relationship with cardiovascular risk, glycemic control, and clinical variables in a well-characterized cohort.

2. Material and Methods

2.1. Patients' Samples

Peripheral blood samples were collected from 128 adult participants, including 96 individuals with type 2 diabetes mellitus (T2DM) and 32 non-diabetic healthy donors. Samples were obtained between August 2018 and December 2024 from the Ambulatory of Stomatological Diseases of the Southwest of Goiás (ADESGO), through a partnership between the Federal University of Jataí (UFJ) and the Municipal Health Secretariat of Jataí, Goiás, as well as from accredited private diagnostic laboratories.

Participants were included according to the following criteria: age ≥ 18 years, ability to undergo fasting blood collection, and signed informed consent. For the T2DM group, a confirmed diagnosis of type 2 diabetes according to ADA criteria was required. For the control group, participants needed to have fasting glucose < 100 mg/dL and no diagnosis of diabetes or chronic metabolic disease. Exclusion criteria for both groups included pregnancy or lactation, type 1 diabetes, active infection or inflammatory disease, malignancy, chronic renal failure (stages III–V), use of corticosteroids or immunosuppressive therapy, hemolyzed or insufficient plasma samples, and incomplete clinical or laboratory data.

The sample size was determined a priori using G*Power 3.1 software, considering a two-tailed t-test, an expected effect size of d = 0.60 for differences in miR-34a expression between groups, a significance level of 0.05, and power of 80%. The minimum required sample size was 108 participants. The final sample of 128 individuals exceeded this requirement, ensuring adequate statistical power. Written informed consent was obtained from all participants prior to inclusion in the study. All

 doi:10.20944/preprints202603.1509.v1

procedures adhered to the Declaration of Helsinki and were approved by the institutional Ethics Committee (CAAE: 69791717.0.0000.5083).

2.2. Clinical, Anthropometric and Metabolic Assessments

Clinical, anthropometric, and biochemical data were obtained when available. Weight, height, and waist circumference were measured using standardized protocols. All blood samples were collected after 12–14 hours of fasting, and participants were instructed to avoid alcohol consumption for at least 72 hours and to refrain from vigorous physical activity prior to sampling. Cardiovascular risk was assessed using the Framingham Risk Score, originally developed by Wilson *et al.* (1998) [13], which incorporates age, sex, total cholesterol, HDL cholesterol, systolic blood pressure, antihypertensive treatment, smoking status, and diabetes status to estimate the 10-year risk of coronary heart disease. Scores were interpreted as follows: <10% (low risk), 10–20% (intermediate risk), and >20% (high risk).

Physical activity levels were assessed using the short version of the International Physical Activity Questionnaire (IPAQ), validated by Craig et al. (2003) [14]. Walking, moderate, vigorous, and total physical activity times were converted into metabolic equivalent values (MET-min/week) using the following coefficients: 3.3 METs for walking, 4.0 METs for moderate activity, and 8.0 METs for vigorous activity. IPAQ results were classified as low (<600 MET-min/week), moderate (600–3000 MET-min/week), or high (>3000 MET-min/week).

2.3. microRNAs and RNA Isolation

Total RNA, including circulating microRNAs, was isolated from 500 µL of plasma using the Norgen® Plasma/Serum Circulating and Exosomal RNA Purification Kit according to the manufacturer's instructions. An exogenous U6 snRNA control (GenBank NM-001207056) was added during extraction for normalization. RNA was eluted in 100 µL of elution buffer. Genomic RNA from peripheral blood cells was extracted using TRIzol® reagent (Invitrogen), and cDNA synthesis was performed from approximately 1 µg of total RNA using the High-Capacity cDNA Reverse Transcription Kit (Thermo Fisher Scientific). Quantitative real-time PCR was conducted in triplicate on a 7500 Real-Time PCR System (Thermo Fisher Scientific). The expression of miR-34a (MIMAT0000260) was normalized to U6 snRNA, and fold changes were calculated using the 2^−ΔΔCq method.

2.4. Protein Biomarkers by Enzyme-Linked Immunosorbent Assay (ELISA)

Peripheral venous blood samples were collected after 12–14 hours of overnight fasting into EDTA-containing tubes and processed within one hour of collection. Samples were centrifuged at 1,500 × g for 15 minutes at 4 °C, and plasma was carefully separated to avoid contamination with cellular components. Aliquots (200–500 µL) were prepared to prevent repeated freeze–thaw cycles and stored at −80 °C until analysis. Before measurement, samples were thawed once on ice, gently mixed, and visually inspected for hemolysis. Hemolyzed samples were excluded from analysis.

Circulating protein levels of SIRT1, IL-6, TNF-α, hs-CRP, VCAM-1, and ICAM-1 were quantified using high-sensitivity sandwich enzyme-linked immunosorbent assay (ELISA) kits, following the manufacturers' instructions. The following commercially available kits were used: Human SIRT1 ELISA Kit (Abcam, Cambridge, UK; Cat# ab171573), Human IL-6 Quantikine HS ELISA Kit (R&D Systems, Minneapolis, MN, USA; Cat# HS600B), Human TNF-α Quantikine HS ELISA Kit (R&D Systems; Cat# HSTA00E), Human hs-CRP ELISA Kit (Thermo Fisher Scientific, Waltham, MA, USA; Cat# EHCRP), Human VCAM-1/CD106 Quantikine ELISA Kit (R&D Systems; Cat# DVC00), and Human ICAM-1/CD54 Quantikine ELISA Kit (R&D Systems; Cat# DCD540).

Standard curves were generated for each analyte using seven-point serial dilutions of recombinant standards supplied with the kits. Concentrations were calculated using a four-parameter logistic (4-PL) regression model. Optical density was measured at 450 nm with wavelength

 doi:10.20944/preprints202603.1509.v1

correction at 570 nm using a BioTek Synergy HTX Multi-Mode Microplate Reader (Agilent Technologies, Santa Clara, CA, USA).

Based on preliminary optimization experiments, plasma samples were diluted as follows: SIRT1 (1:2), IL-6 and TNF-α (undiluted), hs-CRP (1:100), and VCAM-1 and ICAM-1 (1:50), using the assay-specific dilution buffers provided by the manufacturers. All measurements were performed in technical triplicates, and the mean value of the three replicates was used for statistical analysis.

Intra-assay precision was assessed by calculating the coefficient of variation (CV%) for each triplicate set using the formula CV (%) = (standard deviation / mean) × 100. An acceptance threshold of CV < 10% was applied. Samples exceeding this variability threshold were re-analyzed. Inter-assay variability was monitored using internal quality controls included on each plate, and inter-assay CV remained below 12% for all analytes.

To minimize inter-plate variability, samples from controls and T2DM subgroups were randomly distributed across plates. Laboratory personnel performing ELISA analyses were blinded to clinical status and cardiovascular risk classification. Blank wells and internal quality control samples were included in each assay run to ensure consistency and reliability of measurements.

2.5. Oxidative Stress Markers - Malondialdehyde (MDA)

Plasma lipid peroxidation was quantified by measuring malondialdehyde (MDA) using a thiobarbituric acid reactive substances (TBARS) assay. MDA levels were determined using a commercially available TBARS Assay Kit (Cayman Chemical, Ann Arbor, MI, USA; Cat# 10009055), following the manufacturer's instructions.

Briefly, 100 µL of plasma was mixed with sodium dodecyl sulfate (SDS) solution and thiobarbituric acid (TBA) reagent under acidic conditions. The reaction mixture was incubated at 95 °C for 60 minutes to allow formation of MDA–TBA adducts. After cooling on ice for 10 minutes, samples were centrifuged at 1,600 × g for 10 minutes to remove precipitated proteins. The supernatant containing the MDA–TBA chromogen was transferred to a 96-well microplate.

Absorbance was measured at 532 nm using a BioTek Synergy HTX Multi-Mode Microplate Reader (Agilent Technologies, Santa Clara, CA, USA). MDA concentrations were calculated using a standard curve generated from serial dilutions of 1,1,3,3-tetramethoxypropane (TMP), which serves as an MDA precursor standard. A seven-point calibration curve (0–20 µM) was used, and concentrations were interpolated using linear regression.

The assay detection limit was 0.1 µM, with an analytical range of 0.1–20 µM. Results were expressed as nmol/mL of plasma. All samples were analyzed in technical triplicates. Intra-assay precision was assessed by calculating the coefficient of variation (CV%), with an acceptance threshold of CV < 10%. Samples exceeding this threshold were re-analyzed. Inter-assay CV remained below 12%.

2.6. Oxidative Stress Markers - Total Antioxidant Capacity (TAC)

Total antioxidant capacity (TAC) was determined using a Ferric Reducing Antioxidant Power (FRAP)-based method with a commercially available Total Antioxidant Capacity Assay Kit (Abcam, Cambridge, UK; Cat# ab65329). The FRAP assay is based on the reduction of ferric (Fe^{3+}) to ferrous (Fe^{2+}) ions in the presence of antioxidants under acidic conditions. The resulting Fe^{2+}–TPTZ (2,4,6-tripyridyl-s-triazine) complex forms a blue chromophore measurable spectrophotometrically.

Briefly, 20 µL of plasma was mixed with 180 µL of freshly prepared FRAP working reagent containing acetate buffer (300 mM, pH 3.6), TPTZ solution (10 mM in 40 mM HCl), and $FeCl_3 \cdot 6H_2O$ solution (20 mM). The mixture was incubated at 37 °C for 30 minutes in the dark.

Absorbance was measured at 593 nm using a BioTek Synergy HTX Multi-Mode Microplate Reader (Agilent Technologies, USA). TAC values were calculated from a Trolox standard curve (0–2 mM) prepared in parallel with each assay plate. Concentrations were expressed as mmol Trolox equivalents per liter (mmol TE/L). The assay sensitivity was 0.05 mmol/L, with a detection range of 0.05–2.0 mmol/L. All samples were analyzed in technical triplicates, and mean values were used for

 doi:10.20944/preprints202603.1509.v1

statistical analysis. Intra-assay CV was maintained below 8%, and inter-assay CV remained below 10%. Internal quality control samples were included in each plate to monitor assay stability.

2.7. Gene Expression Profile Analysis

Genomic RNA was isolated from peripheral blood cells using TRIZOL® reagent (Invitrogen) according to the manufacturer's recommendations. Complementary DNA (cDNA) was synthesized from ~1µg of total RNA using a High-Capacity cDNA reverse transcription Kit (Thermo Fisher Scientific, Waltham - Massachusetts, EUA), following the manufacturer's instructions. The relative expression level (i.e., fold change) for each gene or miRNA was calculated using the $2^{-\Delta\Delta Cq}$ method. The relative expression of miR-34a (genebank#MIMAT0000260) was normalized to U6 (genebank#NM-001207056) snRNA and analyzed in triplicate on the same MicroAmp optical 96-well plates using a 7500 Real-Time PCR System (Thermo Fisher Scientific, Waltham - Massachusetts, EUA).

2.8. Statistical Analysis of Biomarkers

All statistical analyses were performed using GraphPad Prism version 8.0 (GraphPad Software, San Diego, CA, USA) and supplementary multivariate modeling was conducted using SPSS version 26.0 (IBM Corp., Armonk, NY, USA), when applicable. The distribution of continuous variables was assessed using the Shapiro–Wilk test for normality, complemented by visual inspection of histograms and Q–Q plots.

Homogeneity of variances was evaluated using Levene's test. Normally distributed variables were expressed as mean ± standard deviation (SD), whereas non-normally distributed data were presented as median and interquartile range (IQR). For comparisons between two independent groups, Student's unpaired t-test was applied for normally distributed variables, while the Mann–Whitney U test was used for non-parametric data.

For comparisons among three groups (Control, T2DM–Medium Risk, and T2DM–High Risk), one-way analysis of variance (ANOVA) with Tukey's post hoc test was used for parametric data. When normality assumptions were not met, the Kruskal–Wallis test followed by Dunn's multiple comparison correction was applied. To control for type I error in multiple comparisons across biomarker panels, the false discovery rate (FDR) was adjusted using the Benjamini–Hochberg procedure where appropriate.

Associations between continuous variables (including miR-34a expression, SIRT1 protein levels, inflammatory markers, oxidative stress markers, endothelial dysfunction markers, and cardiovascular risk score) were evaluated using Pearson's correlation coefficient for normally distributed variables and Spearman's rank correlation for non-parametric data. Correlation strength was interpreted according to established thresholds (weak: $r < 0.3$; moderate: 0.3–0.6; strong: > 0.6).

Multivariate linear regression analyses were performed to determine whether SIRT1, miR-34a, and inflammatory markers were independent predictors of cardiovascular risk after adjustment for age, sex, body mass index (BMI), smoking status, dyslipidemia, and HbA1c levels. Standardized beta coefficients (β), 95% confidence intervals (CI), and model R^2 values were reported.

For categorical cardiovascular risk prediction (Medium vs High Risk), logistic regression models were constructed, and odds ratios (OR) with 95% CI were calculated. Model discrimination was evaluated using receiver operating characteristics (ROC) curve analysis and area under the curve (AUC) estimates.

All statistical tests were two-tailed, and a p-value < 0.05 was considered statistically significant.

3. Results

Clinical and metabolic characteristics of the study population are summarized in **Table 1**. A strong association was observed between fasting blood glucose and HbA1c levels, with individuals

 doi:10.20944/preprints202603.1509.v1

presenting fasting glucose ≥200 mg/dL consistently showing HbA1c values >9%, indicative of poor glycemic control.

Table 1. General clinical, anthropometric and biochemical information of the participants based on their diabetes status (n=96).

Variables	n (%)
Age (years)	
< 59	57 (59.3)
≥ 60	39 (40.7)
Sex	
Female	51 (53.1)
Male	45 (46.9)
Smoker	
Yes	33 (34.3)
No	51 (53.1)
Not informed	12 (12.5)
Elitist	
Yes	30 (31.2)
No	51 (53.1)
Not informed	15 (15.6)
Dyslipidemia	
Yes	52 (54.1)
No	44 (45.9)
Steatosis	
Yes	46 (47.9)
No	37 (38.5)
Not informed	13 (13.5)
Fasting blood glucose (mg/dL)	
< 126	13 (13.5)
≥ 126	83 (86.5)
Glycated Hemoglobin (%)	
< 6.5	24 (25.0)
≥ 6.5	72 (75.0)
Cardiovascular risk	
High	49 (51.0)
Medium	47 (49.0)
Overweight	
Yes	51 (53.1)
No	45 (46.9)
Physical activity	
Yes	46 (47.9)
No	50 (52.1)

Cardiovascular risk was significantly associated with lifestyle and metabolic factors. Smoking, dyslipidemia, and hepatic steatosis were more prevalent among individuals classified as high

 doi:10.20944/preprints202603.1509.v1

cardiovascular risk. Additionally, physical inactivity was more frequent in both intermediate- and high-risk groups.

Age was positively associated with cardiovascular risk, with individuals aged ≥65 years more frequently classified in the high-risk category. Sex-stratified analysis revealed heterogeneous distributions, with a subset of female participants exhibiting both poor glycemic control and elevated cardiovascular risk. Based on our investigation diabetes-related health indicators focusing on factors like blood glucose levels, glycated hemoglobin (HbA1c), cardiovascular risk, and their relationships with lifestyle factors such as smoking, physical activity, and comorbid conditions are presented in **Table 1**.

Our results demonstrated that a clear correlation is seen between high fasting blood glucose levels and higher HbA1c percentages. Individuals with fasting blood glucose above 200mg/dL tend to have HbA1c levels exceeding 9%, indicating poor glycemic control. Smoking and dyslipidemia were prevalent among high-risk individuals, suggesting these factors exacerbate cardiovascular complications in diabetic patients.

Physical inactivity was associated with both "medium" and "high" cardiovascular risk categories, highlighting the importance of physical activity in managing diabetes-related risks. Smokers in the dataset predominantly fall into the high-risk category, emphasizing smoking's detrimental effects on cardiovascular and metabolic health. Dyslipidemia and steatosis were common characteristics among individuals with poorly controlled diabetes (HbA1c > 9%). These conditions are likely to contribute to increased cardiovascular risk. Older individuals (65+ years) showed a higher tendency towards high cardiovascular risk, likely due to a cumulative impact of aging, comorbidities, and prolonged diabetes duration. Women in our dataset showed a mix of "medium" and "high" cardiovascular risk, with a notable subgroup exhibiting poor glycemic control.

A correlation analysis among parameters presented (age, sex, smoker, elitist, dyslipidemia, steatosis, fasting blood glucose, glycated hemoglobin (%), overweight and physical activity) related to cardiovascular risk is better represented in **Figure 1.**

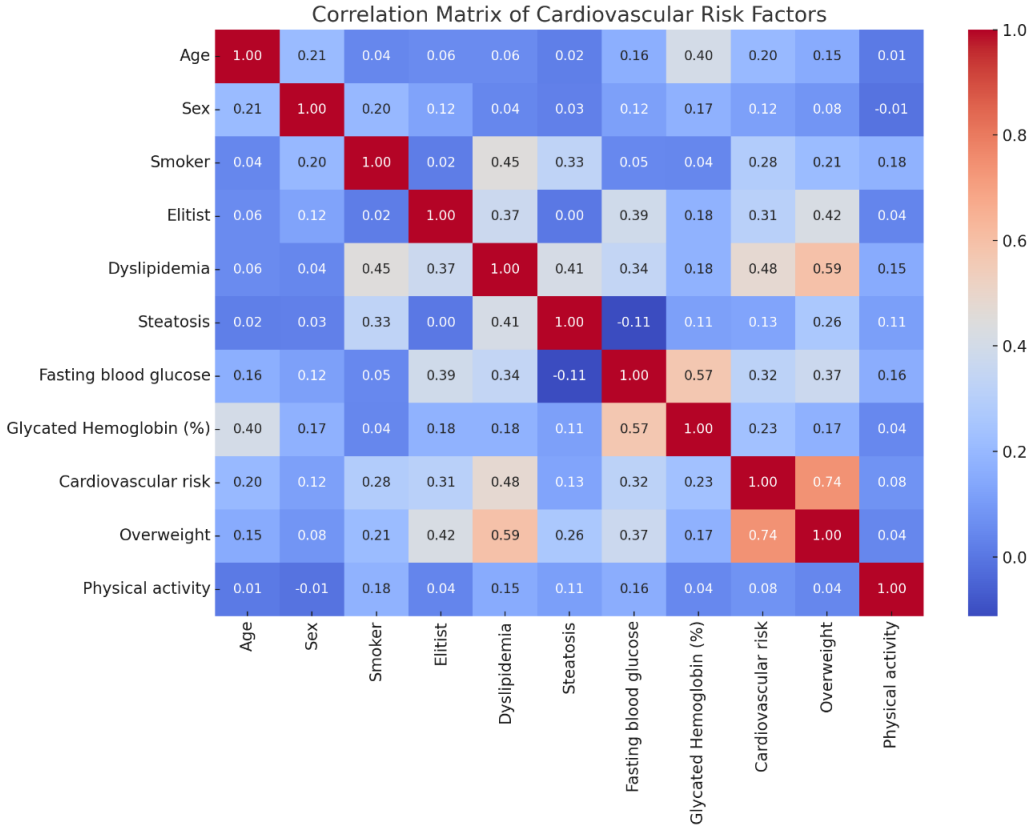

 doi:10.20944/preprints202603.1509.v1

Figure 1. Correlation matrix of cardiovascular risk factors and clinical-metabolic parameters. The heatmap illustrates the pairwise associations among age, sex, smoking status, dyslipidemia, hepatic steatosis, fasting blood glucose, glycated hemoglobin (HbA1c), overweight status, physical activity level, and calculated cardiovascular risk. Correlations were computed using the Pearson correlation test, and the resulting coefficients (r) are represented on a color scale ranging from −1.0 (strong negative correlation) to +1.0 (strong positive correlation). Positive values indicate direct associations between variables, whereas negative values reflect inverse relationships. Color intensity corresponds to the magnitude of the correlation coefficient. All analyses were performed using GraphPad Prism 8.0 (GraphPad Software, USA).

MicroRNA-34a (miR-34a) regulates cell senescence, apoptosis, and inflammatory pathways. Its elevated expression has been linked to cardiovascular diseases due to its role in endothelial dysfunction, inflammation, and lipid metabolism [7,8].

In this study, individuals with type 2 diabetes exhibited significantly higher miR-34a levels compared to non-diabetic controls ($p<0.001$), consistent with their association with inflammatory and metabolic dysregulation in diabetes (**Figure 2A**). Among diabetic individuals, those classified as " T2DM High Risk" showed significantly elevated miR-34a levels compared to the " T2DM Medium Risk " group and non-diabetic controls, highlighting its potential as a biomarker for cardiovascular complications (**Figure 2B**). This is consistent with evidence linking higher miR-34a levels to severe cardiovascular conditions, likely driven by increased endothelial stress and systemic inflammation. Gender-specific analysis revealed distinct miR-34a expression patterns between male and female diabetic individuals, suggesting gender-specific regulatory mechanisms or differences in susceptibility to diabetes-related complications (**Figure 2C**). Non-diabetic controls exhibited the lowest miR-34a levels, representing normal physiological conditions.

In addition to microRNA profiling, we evaluated circulating inflammatory mediators to determine whether systemic inflammation paralleled miR-34a upregulation and cardiovascular risk stratification. As shown in **Table 2**, a progressive and statistically significant increase in inflammatory biomarkers was observed across groups (Controls → T2DM Medium Risk → T2DM High Risk).

Circulating IL-6 levels were significantly elevated in individuals with T2DM compared to controls ($p < 0.001$). Mean IL-6 concentrations increased from 1.82 ± 0.54 pg/mL in controls to 3.45 ± 0.78 pg/mL in the medium-risk group and further to 5.12 ± 1.05 pg/mL in the high-risk group. Post hoc analysis confirmed significant differences between all three groups, demonstrating a clear graded inflammatory response associated with cardiovascular risk severity.

Similarly, TNF-α levels exhibited a stepwise increase across groups (2.95 ± 0.72 pg/mL in controls; 4.88 ± 0.94 pg/mL in medium risk; 6.73 ± 1.12 pg/mL in high risk; $p < 0.001$). The high-risk subgroup showed significantly greater TNF-α concentrations compared to both controls and medium-risk individuals, supporting the presence of amplified inflammatory signaling in patients with more advanced cardiometabolic compromise.

Table 2. Progressive elevation of systemic inflammatory markers according to cardiovascular risk stratification in type 2 Diabetes Mellitus (T2DM).

Inflammatory Markers Results			
Subjects	**Interleukin-6 (IL-6) – pg/mL**	**Tumor Necrosis Factor-α (TNF-α) – pg/mL**	**High-Sensitivity C-Reactive Protein (hs-CRP) – mg/L**
Controls (n = 32)	1.82 ± 0.54	2.95 ± 0.72	1.21 ± 0.63
T2DM – Medium Risk (n = 47)	3.45 ± 0.78	4.88 ± 0.94	3.64 ± 1.08
T2DM – High Risk (n = 49)	5.12 ± 1.05	6.73 ± 1.12	6.42 ± 1.75

 doi:10.20944/preprints202603.1509.v1

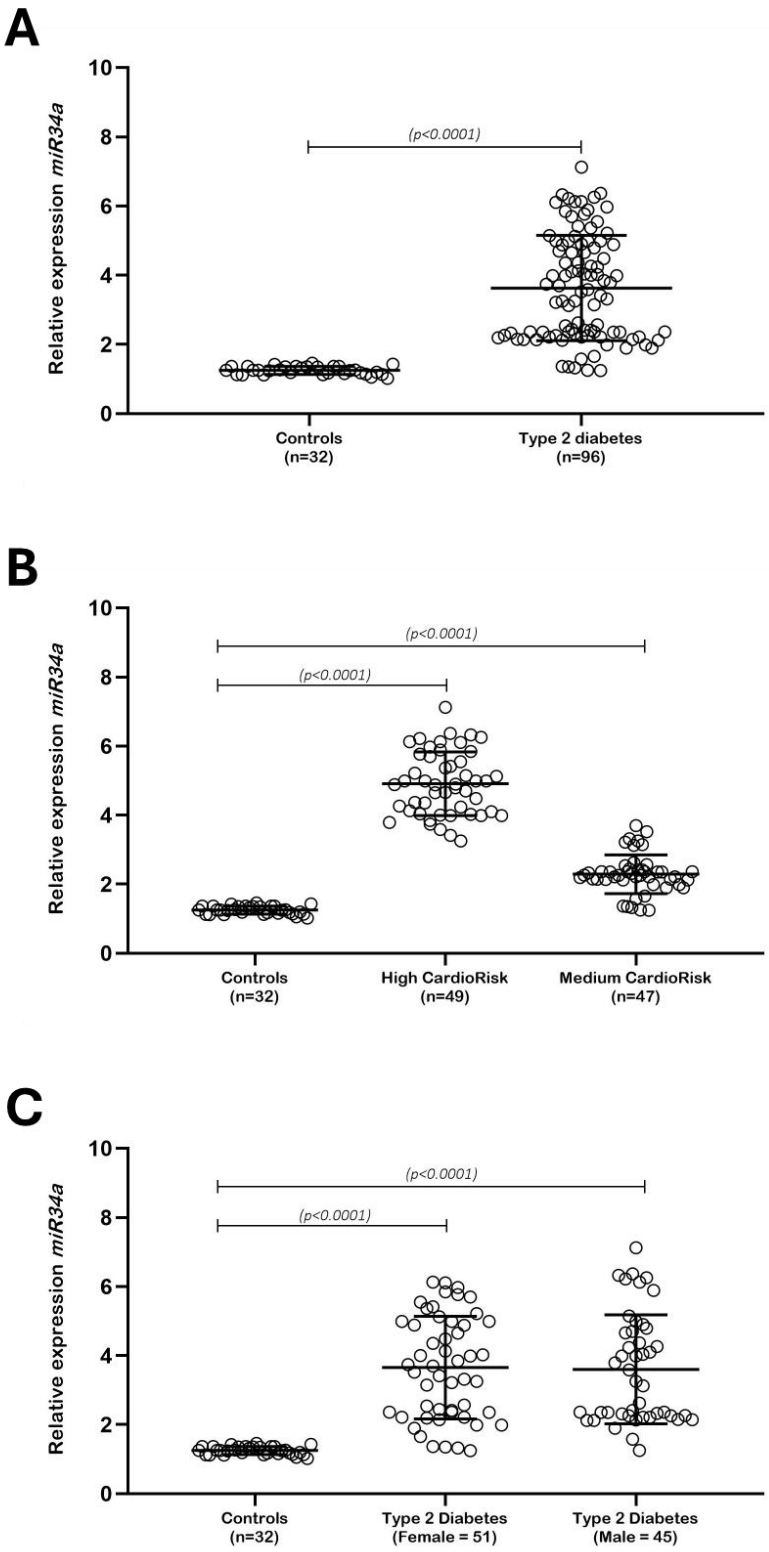

Figure 2. Comparison of miR-34a and expression levels among different diabetic subgroups. (A) Relative expression of miR-34a between controls (non-diabetic individuals, n= 32) and individuals with type 2 diabetes (n=96). (B) Relative expression of miR-34a among controls, diabetic individuals classified as "High cardiac risk", and "Medium" cardiac risk. (C) Relative expression of miR-34a between controls and diabetic individuals stratified by gender. To examine differences between every two groups, Mann-Whitney U test with Bonferroni correction was performed (P value <0.01 was considered significant).

 doi:10.20944/preprints202603.1509.v1

The most pronounced relative difference was observed for hs-CRP, a clinically established marker of cardiovascular inflammation. hs-CRP levels rose from 1.21 ± 0.63 mg/L in controls to 3.64 ± 1.08 mg/L in medium-risk T2DM patients and reached 6.42 ± 1.75 mg/L in high-risk individuals ($p < 0.001$). These values place the high-risk group within a range compatible with significant cardiovascular inflammatory burden, reinforcing the clinical validity of Framingham-based stratification.

Importantly, the inflammatory escalation paralleled the pattern observed for miR-34a expression. Individuals with high cardiovascular risk simultaneously exhibited the highest levels of miR-34a and inflammatory mediators, suggesting convergence of molecular and systemic inflammatory pathways. Given that IL-6 stimulates hepatic CRP synthesis and TNF-α contributes to insulin resistance and endothelial activation, these findings support the hypothesis that miR-34a upregulation may be embedded within a broader pro-inflammatory and pro-atherogenic phenotype in T2DM.

Furthermore, variability (SD) increased in the high-risk group across all inflammatory markers, indicating heterogeneity in inflammatory burden among advanced-risk individuals. This observation suggests that integrating molecular markers such as miR-34a with inflammatory mediators may refine cardiovascular risk stratification beyond traditional clinical parameters.

Collectively, these data demonstrate that T2DM patients classified as high cardiovascular risk exhibit a coordinated increase in miR-34a expression and systemic inflammatory biomarkers, reinforcing the mechanistic link between microRNA dysregulation, inflammation, and cardiovascular vulnerability.

To further characterize the molecular phenotype associated with cardiovascular risk in T2DM, we evaluated systemic oxidative stress markers, including lipid peroxidation and total antioxidant capacity. The results are presented in **Table 3**. A significant and graded increase in oxidative damage was observed across the three groups. Plasma malondialdehyde (MDA) levels, a well-established marker of lipid peroxidation, were significantly elevated in T2DM patients compared to controls (overall $p < 0.001$). Mean MDA concentrations rose from 2.10 ± 0.42 nmol/mL in controls to 3.48 ± 0.63 nmol/mL in the medium cardiovascular risk group and reached 4.92 ± 0.81 nmol/mL in the high-risk group. Post hoc comparisons confirmed significant differences between controls and both diabetic subgroups, as well as between medium- and high-risk individuals, indicating a progressive amplification of oxidative stress in parallel with cardiovascular risk severity.

Table 3. Oxidative stress markers according to cardiovascular risk stratification in individuals with T2DM.

Oxidative Stress Markers Results		
	Malondialdehyde (MDA) – nmol/mL plasma	**Total Antioxidant Capacity (TAC) – mmol Trolox equivalents/L**
Controls (n = 32)	2.10 ± 0.42	1.78 ± 0.28
T2DM – Medium Risk (n = 47)	3.48 ± 0.63	1.32 ± 0.24
T2DM – High Risk (n = 49)	4.92 ± 0.81	0.94 ± 0.19

In contrast, total antioxidant capacity (TAC) exhibited a significant inverse trend (overall $p < 0.001$). Controls displayed the highest antioxidant capacity (1.78 ± 0.28 mmol Trolox equivalents/L), while T2DM individuals showed reduced levels (1.32 ± 0.24 mmol/L in the medium-risk group and 0.94 ± 0.19 mmol/L in the high-risk group). The high-risk subgroup demonstrated an approximate 47% reduction in antioxidant defense compared to controls, suggesting impaired systemic redox buffering capacity.

 doi:10.20944/preprints202603.1509.v1

Notably, the oxidative imbalance closely paralleled the inflammatory pattern described in **Table 2** and the miR-34a expression profile shown in **Figure 2**. Individuals classified as high cardiovascular risk exhibited the highest MDA levels and the lowest TAC values, consistent with a pro-oxidative state accompanying heightened inflammatory activation.

The reciprocal pattern between MDA and TAC reinforces the presence of redox disequilibrium in advanced-risk T2DM patients. Given the established role of SIRT1 in modulating oxidative stress responses and its regulatory interaction with miR-34a, these findings support the concept that miR-34a upregulation may contribute to a coordinated pro-inflammatory and pro-oxidative phenotype that promotes endothelial dysfunction and cardiovascular vulnerability.

Furthermore, increased dispersion of MDA and TAC values in the high-risk group suggests interindividual variability in oxidative burden, highlighting the potential clinical utility of integrating redox biomarkers into multimodal cardiovascular risk assessment models.

Collectively, these results demonstrate that cardiovascular risk progression in T2DM is accompanied by a significant redox imbalance characterized by enhanced lipid peroxidation and reduced antioxidant defense, strengthening the mechanistic link between metabolic dysregulation, oxidative stress, and vascular injury.

To evaluate the discriminatory performance of circulating biomarkers in identifying individuals with high cardiovascular risk among patients with T2DM, receiver operating characteristic (ROC) curve analyses were performed. Circulating miR-34a expression demonstrated good diagnostic accuracy for distinguishing high-risk from medium-risk T2DM individuals, with an area under the curve (AUC) of 0.82 (95% CI: 0.74–0.90; $p < 0.001$). At the optimal cut-off value determined by the Youden index, miR-34a yielded a sensitivity of 78% and specificity of 75%, supporting its potential as a non-invasive biomarker for cardiovascular risk stratification.

SIRT1 protein levels showed an inverse discriminatory pattern, with reduced levels associated with higher cardiovascular risk. ROC analysis revealed an AUC of 0.79 (95% CI: 0.70–0.88; $p < 0.001$), with a sensitivity of 74% and specificity of 72% at the optimal threshold. Among inflammatory markers, hs-CRP exhibited the highest individual predictive performance, with an AUC of 0.87 (95% CI: 0.80–0.94; $p < 0.001$), followed by IL-6 (AUC = 0.84; 95% CI: 0.76–0.91) and TNF-α (AUC = 0.81; 95% CI: 0.73–0.89). These findings reinforce the strong association between systemic inflammation and cardiovascular risk in T2DM. Oxidative stress markers also demonstrated robust predictive capacity. MDA levels yielded an AUC of 0.85 (95% CI: 0.78–0.92; $p < 0.001$), while total antioxidant capacity (TAC) showed an inverse association with risk (AUC = 0.83; 95% CI: 0.75–0.90), indicating that redox imbalance is a key component of cardiovascular vulnerability in diabetic individuals. Endothelial dysfunction markers further contributed to risk discrimination, with VCAM-1 (AUC = 0.84; 95% CI: 0.76–0.91) and ICAM-1 (AUC = 0.82; 95% CI: 0.74–0.89) showing significant predictive value.

Importantly, a combined multi-biomarker model integrating miR-34a, SIRT1, IL-6, MDA, and VCAM-1 significantly improved predictive performance, achieving an AUC of 0.92 (95% CI: 0.86–0.97; $p < 0.001$). This combined model demonstrated superior discrimination compared to any single biomarker alone, with sensitivity of 85% and specificity of 88%, highlighting the advantage of an integrated molecular signature for cardiovascular risk stratification.

To integrate these findings into a unified biological framework, a mechanistic model summarizing the proposed interactions among miR-34a, SIRT1, inflammatory signaling, oxidative stress, and endothelial dysfunction is presented in **Figure 3**. These interconnected processes collectively promote endothelial dysfunction and atherosclerotic progression, ultimately leading to increased cardiovascular risk, as reflected by clinical risk stratification models such as the Framingham Risk Score. This model highlights the miR-34a/SIRT1 regulatory axis as a central integrator of metabolic and vascular alterations in T2DM and supports its potential as a target for biomarker development and therapeutic intervention.

 doi:10.20944/preprints202603.1509.v1

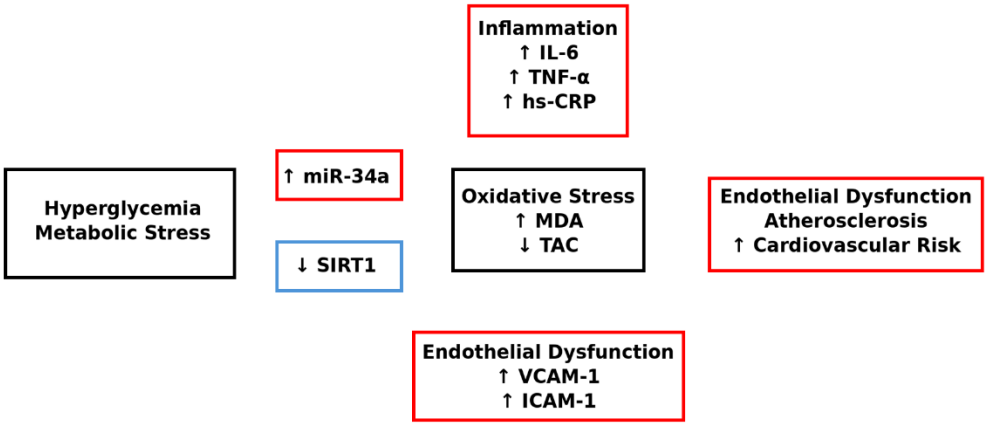

Figure 3. Integrated mechanistic model linking the miR-34a/SIRT1 axis to cardiovascular risk in type 2 diabetes mellitus.

4. Discussion

Type 2 diabetes mellitus (T2DM) is a complex metabolic disorder strongly associated with increased cardiovascular morbidity and mortality, representing one of the leading causes of death worldwide [15]. Chronic hyperglycemia promotes vascular damage through mechanisms involving oxidative stress, formation of advanced glycation end products, and endothelial dysfunction, which are key drivers of atherosclerosis [16,17]. While traditional clinical parameters are useful, they do not fully capture the molecular processes underlying cardiovascular risk, highlighting the need for integrated biomarker approaches.

In the present study, we demonstrate that cardiovascular risk in T2DM is characterized by an integrated molecular signature involving microRNA dysregulation, impaired cytoprotective signaling, systemic inflammation, oxidative stress, and endothelial activation. These findings define a coordinated molecular cascade in which miR-34a upregulation suppresses SIRT1, leading to amplification of inflammatory signaling, oxidative stress, and endothelial activation. Specifically, circulating miR-34a levels were significantly elevated in individuals with T2DM, particularly among those classified as high cardiovascular risk. These findings are consistent with previous studies reporting increased miR-34a expression in metabolic and cardiovascular disorders, where it contributes to endothelial dysfunction, inflammation, and vascular aging [20,22].

Importantly, the upregulation of miR-34a was accompanied by a significant reduction in circulating SIRT1 protein levels, supporting the well-established regulatory interaction between miR-34a and SIRT1 [10,21]. SIRT1 is a NAD^+-dependent deacetylase with critical roles in maintaining endothelial function, reducing oxidative stress, and modulating inflammatory pathways. Experimental studies have demonstrated that miR-34a directly suppresses SIRT1 expression, leading to increased endothelial dysfunction and vascular damage [10,18]. Thus, the inverse relationship observed in our cohort reinforces the concept that miR-34a acts as a central upstream regulator of vascular homeostasis in T2DM.

Beyond microRNA signaling, our results demonstrate a consistent and progressive increase in inflammatory mediators, including IL-6, TNF-α, and hs-CRP, across cardiovascular risk categories. These biomarkers are not only indicators of systemic inflammation but also active contributors to endothelial dysfunction and atherogenesis. IL-6 promotes hepatic CRP synthesis, while TNF-α plays a key role in insulin resistance and vascular inflammation [18,20]. The parallel increase in miR-34a and inflammatory markers suggests that miR-34a may be embedded within a broader pro-inflammatory regulatory network, amplifying vascular injury in T2DM.

In addition, oxidative stress analysis revealed a pronounced imbalance between pro-oxidant and antioxidant systems. Elevated levels of malondialdehyde (MDA) and reduced total antioxidant capacity (TAC) were observed in high-risk individuals, indicating enhanced lipid peroxidation and

 doi:10.20944/preprints202603.1509.v1

impaired antioxidant defense. These findings are consistent with previous reports demonstrating that oxidative stress is a major contributor to vascular damage in diabetes and atherosclerosis [17,18]. Given the established role of SIRT1 in regulating oxidative stress responses, its downregulation may directly contribute to the observed redox imbalance, further linking miR-34a dysregulation to oxidative damage.

Endothelial dysfunction markers, including VCAM-1 and ICAM-1, were also significantly elevated in individuals with high cardiovascular risk. These adhesion molecules play a critical role in leukocyte recruitment and vascular inflammation, representing early events in atherogenesis. Their increased expression reflects endothelial activation and damage, which are central features of diabetic vascular complications [11]. The association of these markers with inflammatory and oxidative pathways suggests that endothelial dysfunction represents a downstream consequence of the integrated molecular disturbances identified in this study.

Taken together, our findings support a mechanistic cascade in which miR-34a upregulation leads to SIRT1 suppression, triggering a coordinated increase in inflammation, oxidative stress, and endothelial dysfunction. This integrated pathway provides a biologically plausible explanation for the increased cardiovascular risk observed in T2DM and aligns with previous mechanistic studies demonstrating the role of the miR-34a/SIRT1 axis in vascular pathology [10,21].

From a clinical perspective, these findings are highly relevant. The combined assessment of miR-34a, SIRT1, and associated inflammatory, oxidative, and endothelial markers may offer a non-invasive and integrative strategy for early identification of high-risk individuals. Importantly, this molecular panel may capture subclinical pathophysiological alterations not detectable by traditional clinical parameters, thereby improving cardiovascular risk stratification and enabling more personalized therapeutic approaches.

Despite these strengths, several limitations should be acknowledged. First, the cross-sectional design precludes causal inference between miR-34a dysregulation and cardiovascular outcomes. Second, the study population was derived from a single geographic region, which may limit generalizability. Third, although strong associations were identified, functional experiments were not performed to directly validate mechanistic pathways. Finally, the absence of longitudinal follow-up prevents evaluation of the predictive value of these biomarkers over time. Future studies should include multicenter cohorts, longitudinal designs, and experimental validation to further elucidate these relationships.

In conclusion, this study demonstrates that cardiovascular risk in T2DM is associated with a coordinated molecular signature involving miR-34a upregulation, SIRT1 suppression, systemic inflammation, oxidative stress, and endothelial dysfunction. These findings support the potential of integrated biomarker panels in precision cardiometabolic medicine and provide a framework for future translational and clinical investigations.

Authors contribution: FMO: Wrote the manuscript with input from all authors. Planned the experiments; FSN: Planned and performed the experiments; EVF: Discussed the results and contributed to the final manuscript; MB: Discussed the results and contributed to the final manuscript; DMO: Discussed the results and contributed to the final manuscript; CSS: Supervised the findings of this work.

Declaration of funding: Association for Health Education & Research, Brazil. Genomic Medicine Study Group (GMEG).

Ethics Statement: This study was approved by the Research Ethics Committee of the Federal University of Jataí, Brazil (69791717.0.0000.5083).

Consent: Written informed consent was obtained from the patient and her parents.

Data Availability Statement: Research data are not shared.

Acknowledgments: Research group in Molecular Epidemiology (EPIMOL), CNPq, Brazil. Association for Health Education & Research, Brazil. Genomic Medicine Study Group (GMEG).

 doi:10.20944/preprints202603.1509.v1

Disclosure statement: No potential conflict of interest was reported by the author(s).

References

1. Piché ME, Tchernof A, Després JP. Obesity phenotypes, diabetes, and cardiovascular diseases. Circ Res. 2020 May 22;126(11):1477–500. doi:10.1161/CIRCRESAHA.120.316101
2. Liu Z, Wang H, Yang Z, Lu Y, Zou C. Causal associations between type 1 diabetes mellitus and cardiovascular diseases: a Mendelian randomization study. Cardiovasc Diabetol. 2023;22:236. doi:10.1186/s12933-023-01974-6
3. Yun JS, Ko SH. Current trends in epidemiology of cardiovascular disease and cardiovascular risk management in type 2 diabetes. Metabolism. 2021 Oct;123:154838. doi:10.1016/j.metabol.2021.154838
4. Ma CX, Ma XN, Guan CH, Li YD, Mauricio D, Fu SB. Cardiovascular disease in type 2 diabetes mellitus: progress toward personalized management. Cardiovasc Diabetol. 2022;21:74. doi:10.1186/s12933-022-01450-7
5. Martinez M, Santamarina J, Pavesi A, Musso C, Umpierrez GE. Glycemic variability and cardiovascular disease in patients with type 2 diabetes. BMJ Open Diabetes Res Care. 2021;9:e002032. doi:10.1136/bmjdrc-2020-002032
6. Li WJ, Wang Y, Liu R, Kasinski AL, Shen H, Slack FJ, Tang DG. MicroRNA-34a: potent tumor suppressor, cancer stem cell inhibitor, and potential anticancer therapeutic. Front Cell Dev Biol. 2021;9:640587. doi:10.3389/fcell.2021.640587
7. Thounaojam MC, Bartoli M. MicroRNA-34a and vascular senescence in diabetes. Aging (Albany NY). 2019;11(24):11799–800. doi:10.18632/aging.102622
8. Hua CC, Liu XM, Liang LR, Wang LF, Zhong JC. Targeting the microRNA-34a as a novel therapeutic strategy for cardiovascular diseases. Front Cardiovasc Med. 2022;8:784044. doi:10.3389/fcvm.2022.784044
9. Chen Q, Shen Z, Mao Y, Li Q, Liu Y, Mei M, et al. Inhibition of microRNA-34a mediates protection of thymosin beta 4 in endothelial progenitor cells against advanced glycation end-products by targeting B-cell lymphoma 2. Can J Physiol Pharmacol. 2019;97(10):945–51. doi:10.1139/cjpp-2018-0620
10. Zhang F, Cui J, Liu X, Lv B, Liu X, Xie Z, Yu B. Roles of microRNA-34a targeting SIRT1 in mesenchymal stem cells. Stem Cell Res Ther. 2015;6:195. doi:10.1186/s13287-015-0200-5
11. Okonkwo UA, DiPietro LA. Diabetes and wound angiogenesis. Int J Mol Sci. 2017;18(7):1419. doi:10.3390/ijms18071419
12. Li Q, Kim YR, Vikram A, Kumar S, Kassan M, Gabani M, et al. P66Shc-induced microRNA-34a causes diabetic endothelial dysfunction by downregulating sirtuin 1. Arterioscler Thromb Vasc Biol. 2016;36(12):2394–403. doi:10.1161/ATVBAHA.116.308808
13. Iadecola C, Parikh NS. Framingham General Cardiovascular Risk Score and cognitive impairment: the power of foresight. J Am Coll Cardiol. 2020;75(20):2535–7. doi:10.1016/j.jacc.2020.03.081
14. Matsudo S, Araújo T, Matsudo V, Andrade D, Andrade E, de Oliveira L, Braggion G. International Physical Activity Questionnaire (IPAQ): study of validity and reliability in Brazil. Rev Bras Ativ Fís Saúde. 2001;6(2):5–18. doi:10.12820/rbafs.v6i2.1269
15. Hitsumoto T. Clinical significance of cardio-ankle vascular index as a cardiovascular risk factor in elderly patients with type 2 diabetes mellitus. J Clin Med Res. 2018;10(4):330–6. doi:10.14740/jocmr3348w
16. Viigimaa M, Sachinidis A, Toumpourleka M, Koutsampasopoulos K, Alliksoo S, Titma T. Macrovascular complications of type 2 diabetes mellitus. Curr Vasc Pharmacol. 2020;18(2):110–6. doi:10.2174/1570161117666190425112753
17. Priya HK, Jha KP, Kumar N, Singh S. Reactive oxygen species and mitochondrial calcium's roles in the development of atherosclerosis. Curr Pharm Des. 2024;30(23):1812–21. doi:10.2174/1381612829666240318112045
18. Batty M, Bennett MR, Yu E. The role of oxidative stress in atherosclerosis. Cells. 2022;11(23):3843. doi:10.3390/cells11233843
19. Chen P, Chen F, Lei J, Li Q, Zhou B. Activation of the miR-34a-mediated SIRT1/mTOR signaling pathway by urolithin A attenuates D-galactose-induced brain aging in mice. Neurotherapeutics. 2019;16(4):1269–82. doi:10.1007/s13311-019-00735-8

 doi:10.20944/preprints202603.1509.v1

20. Jianbing H, Xiaotian L, Jie T, Xueying C, Honge J, Bo Z, et al. The effect of allograft inflammatory factor-1 on inflammation, oxidative stress, and autophagy via miR-34a/ATG4B pathway in diabetic kidney disease. Oxid Med Cell Longev. 2022;2022:1668000. doi:10.1155/2022/1668000
21. Zhu H, Lin Y, Liu Y. miR-34a increases inflammation and oxidative stress levels in patients with necrotizing enterocolitis by downregulating SIRT1 expression. Mol Med Rep. 2021;24(3):664. doi:10.3892/mmr.2021.12459
22. Liang M, Shao A, Tang X, Feng M, Wang J, Qiu Y. MiR-34a affects dexmedetomidine-inhibited chronic inflammatory visceral pain by targeting HDAC2. BMC Anesthesiol. 2019;19:131. doi:10.1186/s12871-019-0810-7
23. Wu J, Liang W, Tian Y, Ma F, Huang W, Jia Y, et al. Inhibition of p53/miR-34a improves diabetic endothelial dysfunction via activation of SIRT1. J Cell Mol Med. 2019;23(5):3538–48. doi:10.1111/jcmm.14291
24. Kaur P, Kotru S, Singh S, Munshi A. Role of miRNAs in diabetic neuropathy: mechanisms and possible interventions. Mol Neurobiol. 2022;59(3):1836–49. doi:10.1007/s12035-021-02517-5